Title

B lymphocytes trigger monocyte mobilization and impair heart function after acute myocardial infarction

Journal

Nature Medicine, 19(10)

ISSN

1078-8956

Authors

Zouggari, Yasmine
Ait-Oufella, Hafid
Bonnin, Philippe
et al.

Publication Date

2013-10-01

DOI

10.1038/nm.3284

Peer reviewed

Published in final edited form as:
Nat Med. 2013 October ; 19(10): 1273–1280. doi:10.1038/nm.3284.

B lymphocytes trigger monocyte mobilization and impair heart function after acute myocardial infarction

Yasmine Zouggari[1,2,13], **Hafid Ait-Oufella**[1,2,3,13], **Philippe Bonnin**[4], **Tabassome Simon**[3,5], **Andrew P Sage**[6], **Coralie Guérin**[1,2], **José Vilar**[1,2], **Giuseppina Caligiuri**[7], **Dimitrios Tsiantoulas**[8,9], **Ludivine Laurans**[1,2], **Edouard Dumeau**[1,2], **Salma Kotti**[5], **Patrick Bruneval**[1,2,10], **Israel F Charo**[11], **Christoph J Binder**[8,9], **Nicolas Danchin**[10], **Alain Tedgui**[1,2], **Thomas F Tedder**[12], **Jean-Sébastien Silvestre**[1,2,13], and **Ziad Mallat**[1,6,13]

[1]Institut National de la Santé et de la Recherche Médicale (INSERM), Unit 970, Paris Cardiovascular Research Center, Paris, France

[2]Université Paris-Descartes, Paris, France

[3]Assistance Publique, Hôpitaux de Paris, Université Pierre et Marie Curie, Paris, France

[4]Université Paris-Diderot, Sorbonne Paris Cité, INSERM, Unit 965, Assistance Publique Hôpitaux de Paris, Hôpital Lariboisière, Paris, France

[5]Unité de Recherche Clinique de L'Est Parisien, Hôpital Saint Antoine, Paris, France

[6]Division of Cardiovascular Medicine, University of Cambridge, Addenbrooke's Hospital, Cambridge, UK

[7]INSERM, Unit 698, Paris, France

[8]Department of Laboratory Medicine, Medical University of Vienna, Austria

[9]Center for Molecular Medicine, Austrian Academy of Sciences, Vienna, Austria

[10]Assistance Publique, Hôpitaux de Paris, Hôpital Européen Georges Pompidou, Université Paris-Descartes, Paris, France

[11]Gladstone Institute of Cardiovascular Disease, San Francisco, California, USA

Correspondence should be addressed to Z.M. (zm255@medschl.cam.ac.uk).
[13]These authors contributed equally to this work.

Note: Any Supplementary Information and Source Data files are available in the online version of the paper.

AUTHOR CONTRIBUTIONS

Y.Z. and H.A.-O. performed the experiments and acquired and interpreted the data. P. Bonnin performed and interpreted the ultrasound studies. T.S. and N.D. were responsible for the FAST-MI cohort and interpreted the statistical data. A.P.S. contributed to the Baff and Baff-r studies. C.G. contributed to flow cytometry analysis and interpretation. J.V. and E.D. contributed to data acquisition and analysis. G.C. and L.L. performed the biomarkers measurements. D.T. and C.J.B. were involved in antibody measurements and Baff-specific antibody experiments. S.K. performed the statistical analysis on the human data. P. Bruneval analyzed and interpreted the disease pathology. I.F.C. provided the *Ccl7*$^{-/-}$ mice. A.T. contributed to study design and data interpretation. T.F.T. generated and provided the CD20 mAb. J-S.S. and Z.M. designed the experiments, analyzed and interpreted the data. Y.Z., J.-S.S. and Z.M. wrote the manuscript.

COMPETING FINANCIAL INTERESTS

The authors declare no competing financial interests.

[12]Department of Immunology, Duke University Medical Center, Durham, North Carolina, USA

Abstract

Acute myocardial infarction is a severe ischemic disease responsible for heart failure and sudden death. Here, we show that after acute myocardial infarction in mice, mature B lymphocytes selectively produce Ccl7 and induce Ly6C^{hi} monocyte mobilization and recruitment to the heart, leading to enhanced tissue injury and deterioration of myocardial function. Genetic (Baff receptor deficiency) or antibody-mediated (CD20- or Baff-specific antibody) depletion of mature B lymphocytes impeded Ccl7 production and monocyte mobilization, limited myocardial injury and improved heart function. These effects were recapitulated in mice with B cell–selective *Ccl7* deficiency. We also show that high circulating concentrations of CCL7 and BAFF in patients with acute myocardial infarction predict increased risk of death or recurrent myocardial infarction. This work identifies a crucial interaction between mature B lymphocytes and monocytes after acute myocardial ischemia and identifies new therapeutic targets for acute myocardial infarction.

Acute thrombotic obstruction of the blood flow in coronary arteries precipitates myocardial infarction, with deleterious consequences on heart function[1–4]. The mainstay of treatment involves rapid restoration of a patent coronary artery either mechanically or through thrombolytic and antiplatelet therapies and administration of agents that reduce oxygen consumption and protect the heart muscle[1,5]. Still, the clinical and socio-economic burden of ischemic heart disease is unacceptably high, and the efficacy of multiantithrombotic therapies is often mitigated by an increased risk of hemorrhagic events. Thus, efforts are being directed toward targeting other pathophysiological pathways, particularly those involved in postischemic cardiac remodeling[4,6].

The immune system becomes activated in response to myocardial damage[7]. Shortly after ischemia, the damaged tissue exposes ligands (for example, non-myosin heavy chain type IIA and C) that are recognized by components of the innate immune system, which leads to its activation[8–12]. C-reactive protein, a short pentraxin acute-phase protein, also binds damaged tissue and activates complement, leading to aggravation of tissue injury in the setting of acute myocardial infarction[13]. In contrast, long pentraxin 3, a molecule that limits complement activation, has a cardioprotective role in this setting[14]. The acute inflammatory response also leads to the mobilization and recruitment of innate immune cells. A few hours after the ischemic insult, neutrophils are actively recruited into the ischemic tissue and contribute to tissue inflammation and cardiovascular injury through the production of inflammatory mediators, reactive oxygen species and various proteases[15,16]. This wave of neutrophil infiltration is followed by the mobilization and recruitment of monocytes. Recent studies have shed light on the mechanisms by which monocytes are recruited to the heart and the life cycle of the recruited monocytes in the setting of acute myocardial infarction. These studies have suggested that Ly6C^{hi} and Ly6C^{lo} monocytes have pathogenic and protective roles, respectively, in cardiac remodeling and preservation of heart function[17,18].

Whether targeting the immune response in acute myocardial infarction would be beneficial is still uncertain. Attempts to target the complement pathway have not been efficacious in patients with acute myocardial infarction[19–22]. Better characterization of the immune

response following ischemic injury and the mechanisms by which it contributes to tissue damage is therefore required to fill the existing gap of knowledge that limits clinical translation.

Here, we addressed the role of mature B lymphocytes, a subset of immune cells that orchestrates a variety of adaptive immune responses relevant to human diseases[23] but that has relatively been neglected in the setting of ischemic injury. We show that after acute myocardial infarction in mice, mature B lymphocytes are activated to produce Ccl7, a chemokine that induces monocyte mobilization from the bone marrow, leading to enhanced myocardial inflammation, tissue injury and deterioration of myocardial function.

RESULTS

Mature B cells are recruited to the ischemic myocardium

To identify the inflammatory cell repertoire within the injured myocardium, we induced acute myocardial infarction in C57BL/6J mice by permanent coronary artery ligation and analyzed cell suspensions of digested infarcts at different time points by flow cytometry. We found that neutrophil counts ($CD11b^{+}Ly6G^{hi}7/4^{hi}$ cells; 7/4 refers to antibody clone 7/4 directed against the Ly-6B.2 alloantigen, whose staining is equivalent to staining with Ly6C) peaked at day 1 after myocardial infarction (**Supplementary** Fig. 1a), followed by successive waves of $7/4^{hi}$ ($Ly6C^{hi}$) and $7/4^{lo}$ ($Ly6C^{lo}$) monocytes ($CD11b^{hi}Ly6G^{-}$) (**Supplementary** Fig. 1b) and by accumulation of dendritic cells, macrophages and natural killer cells (**Supplementary** Fig. 1c,**d**). We also found that $CD3^{+}$ T lymphocytes accumulated in the injured myocardium within 1 d after myocardial infarction and their numbers dropped thereafter (**Supplementary** Fig. 1e). These results are in agreement with previous studies[17].

We next characterized B lymphocyte infiltration into the ischemic cardiac tissue. After myocardial infarction, B lymphocytes, defined as $B220^{+}IgM^{+}$ cells, accumulated in the infarct area, with a peak in their numbers on day 5 after infarction. Their numbers waned thereafter to levels comparable to those in sham-operated mice (**Supplementary** Fig. 2a). Immunohistological and additional flow cytometry analyses confirmed the increased numbers of both $B220^{+}$ and $CD19^{+}IgD^{+}IgM^{low}$ B lymphocytes in the border infarct area compared to their numbers in cardiac tissue from sham-operated mice (**Supplementary** Fig. 2b,**c**). Thus, myocardial infarction triggers the infiltration of circulating mature B lymphocytes into cardiac tissue, suggesting a potential role of B cell–mediated immune response in this setting.

B cell depletion improves cardiac function

To directly assess the role of mature B lymphocytes in cardiac remodeling after myocardial infarction, we depleted B lymphocytes using a CD20-specific monoclonal antibody (CD20 mAb)[24,25]. As expected, we found that CD20 mAb treatment led to a sustained and profound reduction of the number of mature B lymphocytes in cardiac tissue (**Supplementary** Fig. 3a), peripheral blood (Fig. 1a) and spleen (**Supplementary** Fig. 3b).

Both follicular and marginal zone B cells were depleted (**Supplementary** Fig. 3c, whereas B1 cells were preserved during the duration of the experiment (data not shown)[26].

We next assessed cardiac function by echocardiography 14 d after myocardial infarction. CD20 mAb–induced B cell depletion led to a smaller end-systolic left ventricular dimension ($P = 0.016$), a significant improvement of left ventricular fractional shortening ($P = 0.021$) and increased left ventricular myocardial contractility ($P = 0.025$) compared to PBS-treated control mice (Fig. 1b). This treatment also led to a smaller infarct size ($P = 0.024$) and less interstitial fibrosis as assessed by collagen content ($P = 0.016$) (Fig. 1c). In addition, B cell depletion reduced the number of apoptotic cells within the injured myocardium, as shown by TUNEL staining ($P = 0.005$), but had no effect on neovascularization (**Supplementary** Fig. 4). Overall, these results show that systemic B cell depletion significantly reduces post-ischemic injury, prevents adverse ventricular remodeling and improves cardiac function after acute myocardial infarction.

B cell depletion reduces proinflammatory responses

Previous studies reported a pathogenic role for natural IgM antibodies in the first 24 h after ischemia-reperfusion injury[11,27]. To address potential mechanisms involved in B cell–mediated effects on cardiac remodeling and function, we assessed changes in antibody production after CD20 mAb treatment. Depletion of mature B cells did not alter IgM or IgG abundance in the first 3 d after myocardial infarction (**Supplementary** Fig. 5), arguing against an antibody-mediated effect. The moderate decrease of IgM levels observed at day 14 after myocardial infarction in CD20 mAb–treated mice (**Supplementary** Fig. 5) might be secondary to the reduction of myocardial necrosis.

We next assessed changes in the inflammatory response. Treatment with CD20 mAb resulted in markedly lower levels of both systemic and local proinflammatory cytokines measured at day 14 after myocardial infarction (Fig. 1d and **Supplementary** Fig. 6a,*b*). Interleukin-1β (IL-1β*; P* = 0.04), tumor necrosis factor-α (TNF-α; $P = 0.004$) and IL-18 ($P = 0.041$) mRNA levels were significantly lower in infarcted hearts of B cell depleted–mice compared to the control group (Fig. 1d). In contrast, expression of the anti-inflammatory mediators IL-10 and TGF-β were not significantly affected in the B cell–depleted mice (Fig. 1d). We observed similar results in spleens and lymph nodes of B cell–depleted mice (**Supplementary** Fig. 6a,**b**), suggesting a blunted inflammatory response.

B cell depletion alters monocyte compartmentalization

We next sought to address the mechanisms that could account for the reduced inflammatory response and the improvement in ventricular remodeling after CD20 mAb treatment. B cell–depleted mice showed altered monocyte compartmentalization after acute myocardial infarction, as revealed by enhanced accumulation of $7/4^{hi}$ monocytes in the bone marrow ($P = 0.01$ versus PBS-treated controls) (Fig. 2a) and the spleen ($P = 0.02$ versus PBS-treated controls) (**Supplementary Fig. 7**), associated with a significant decrease of $7/4^{hi}$ monocyte circulating blood counts ($P = 0.015$ versus PBS-treated controls) (Fig. 2b). These results suggest that B cell depletion impairs monocyte mobilization after acute myocardial infarction.

We also addressed the effect of CD20-mediated B cell depletion on monocyte recruitment from the circulating blood into the ischemic heart. Mice underwent coronary artery ligation and 1 h after ligation were treated with either PBS or CD20 mAb. Four hours after ligation, the two groups of mice received an intravenous infusion of $CD45.1^+$ bone marrow–derived mononuclear cells (15×10^6) isolated from wild-type (WT) mice, and we quantified the number of recruited $CD45.1^+CD11b^+Ly6G^-Ly6C^+$ cells in the myocardium 3 d after monocyte transfer. CD20-mediated B cell depletion led to a substantial reduction in monocyte recruitment into the ischemic myocardium (Fig. 2c). We also found a nonsignificant trend toward reduced accumulation of $7/4^{hi}$ monocytes 3 d after CD20 mAb treatment (**Supplementary Fig. 8a**) and a substantial reduction of macrophage accumulation within the ischemic heart 5 d after CD20 mAb treatment (Fig. 2d). Other cell subsets were not altered (**Supplementary Fig. 8b**,**c**).

B lymphocytes produce Ccl7 and trigger monocyte migration

Given that Ccr2-mediated signals are required for monocyte mobilization from the bone marrow[17,28] and recruitment into injured tissues, we examined potential changes in the production of Ccl2 and Ccl7, the two major Ccr2 ligands. We found that acute myocardial infarction led to substantial increases of Ccl2 and Ccl7 mRNA and protein levels in blood and cardiac tissue (**Supplementary Fig. 9**). Notably, B cell depletion was associated with a significant and selective impairment of Ccl7 protein levels ($P = 0.03$) compared to the control group, whereas Ccl2 (and Ccl12) levels were not significantly affected by B cell depletion (Fig. 3a and **Supplementary Fig. 9**).

These results suggest that B lymphocytes might produce Ccl7 to mobilize monocytes. To address this hypothesis, we first evaluated Ccl7 expression by splenic B cells using flow cytometry and reverse-transcription quantitative PCR (RT-qPCR). We found that $CD19^+$ B lymphocytes, which are markedly depleted after CD20 mAb treatment, express Ccl7, with higher expression after myocardial infarction (**Supplementary Fig. 10**). Splenic B cells from *Myd88*$^{-/-}$; *Trif*$^{-/-}$ mice, which cannot respond to Toll-like receptor (TLR) signaling, produced substantially less Ccl7 than did splenic B cells from WT mice at day 1 after myocardial infarction (**Supplementary Fig. 10**), suggesting at least a partial dependence on TLR signaling. We also assessed Ccl7 secretion by cultured splenic B lymphocytes isolated from WT mice. Whereas Ccl2 and Ccl12 were undetectable in the supernatants of B lymphocytes from WT mice (data not shown), these cells produced a substantial amount of Ccl7 that was further increased after their activation with CD40-specific and IgM-specific antibodies (data not shown) or with TLR agonists, particularly CpG (Fig. 3b and **Supplementary Fig. 10**). Control oligodeoxynucleotides, which are unable to stimulate TLRs, did not induce Ccl7 production (data not shown). We also found that activated cultured B lymphocytes strongly enhanced $7/4^{hi}$ monocyte transmigration *in vitro* compared to nonstimulated B lymphocytes ($P < 0.0001$) (Fig. 3c). Notably, neutralizing antibody to Ccl7 abrogated B cell–induced migration of cultured $7/4^{hi}$ monocytes ($P = 0.0003$), whereas Ccl2 neutralization had no effect (Fig. 3c).

Ccl7-deficient B cells fail to affect cardiac function

These findings prompted us to investigate the direct role of B cell–derived Ccl7 in post-ischemic cardiac remodeling. First, we studied the role of Ccl7 in this setting using Ccl7-deficient mice. We found that after acute myocardial infarction, Ccl7 deficiency was associated with a reduction of $7/4^{hi}$ monocyte mobilization from the bone marrow (P = 0.013 versus WT) to the blood (P = 0.04 versus WT) and improvement of cardiac function (**Supplementary Fig. 11**). To further substantiate the role of B cell–derived Ccl7 in this setting, we injected *Rag1*$^{-/-}$ mice (lacking B and T cells) with either WT splenocytes, B cell–depleted splenocytes or B cell–depleted splenocytes resupplemented with WT or *Ccl7*$^{-/-}$ B lymphocytes. The purity of the B lymphocytes is shown in **Supplementary Figure 12**. We first verified that resupplementation with WT or *Ccl7*$^{-/-}$ B lymphocytes substantially increased B cell numbers in the spleens of *Rag1*$^{-/-}$ mice compared to mice injected with B cell–depleted splenocytes only (**Supplementary Fig. 12**). Resupplementation with WT B lymphocytes was associated with higher circulating Ccl7 concentrations compared to mice receiving B cell–depleted splenocytes only (968.5 ± 46.06 pg ml^{-1} and 201.1 ± 28.31 pg ml^{-1}, respectively, P < 0.0001). In contrast, resupplementation of B cell–depleted splenocytes with B lymphocytes isolated from *Ccl7*$^{-/-}$ mice failed to increase Ccl7 concentrations (152.6 ± 39.9 pg ml^{-1}, P < 0.0001 versus WT B lymphocytes). We also found that resupplementation with WT B lymphocytes was associated with higher $7/4^{hi}$ monocyte numbers in the blood and within the injured myocardium compared to the group receiving B cell–depleted splenocytes only (Fig. 3d), an effect that was abrogated in mice resupplemented with *Ccl7*$^{-/-}$ B lymphocytes (Fig. 3d). Thus, B cell–derived Ccl7 triggers selective mobilization and tissue recruitment of $7/4^{hi}$ monocytes after acute myocardial infarction.

We next examined the consequences of Ccl7 deficiency in B lymphocytes on post-ischemic cardiac remodeling. We found that transfer of B cell–depleted splenocytes into *Rag1*$^{-/-}$ mice reduced end-systolic left ventricular chamber dimension (P = 0.04) and improved left ventricular fractional shortening (P = 0.008) after myocardial infarction compared to transfer of nondepleted splenocytes (Fig. 4a). This effect was abrogated after resupplementation of B cell–depleted splenocytes with B lymphocytes isolated from WT mice (P = 0.0007 and P = 0.02, respectively) but was not altered after resupplementation with *Ccl7*$^{-/-}$ B lymphocytes (Fig. 4a). B cell depletion also reduced infarct size (P = 0.04; Fig. 4b) and collagen content (Fig. 4c); these effects were blunted by resupplementation with WT but not with *Ccl7*$^{-/-}$ B lymphocytes (Fig. 4b,c). Circulating IgM and IgG concentrations were similar in mice resupplemented with WT versus *Ccl7*$^{-/-}$ B lymphocytes (**Supplementary Fig. 12**), making a contribution of humoral immunity to the cardioprotective effect unlikely, although we did not measure specific antibody titers.

We also generated a B cell–restricted Ccl7-deficient mouse model by reconstituting lethally irradiated WT mice with a mixture of bone marrow from μMT (B cell-deficient) and *Ccl7*$^{-/-}$ mice (see Online Methods). The control group received a mixture of μMT and *Ccl7*$^{+/+}$ bone marrow. Again, we found that restricted Ccl7 deficiency in B lymphocytes led to a reduction of circulating Ccl7 concentrations (Fig. 4d) and improved heart function after acute myocardial infarction (Fig. 4e).

Role of Baff signaling in post-ischemic myocardial injury

Baff signaling through Baff receptor (Baff-r, encoded by *Tnfrsf13c*) is required for the maintenance of mature B2 cells, and Baff-r deficient (*Tnfrsf13c*$^{-/-}$) mice are characterized by a profound reduction of follicular and marginal zone B lymphocytes but preservation of B1 cells[29] (**Supplementary Fig. 13**). We therefore addressed the impact of Baff-r deficiency on the pathophysiology of post-ischemic myocardial injury. We found that *Tnfrsf13c*$^{-/-}$ mice showed significantly more accumulation of Ly6C^{hi} monocytes in the bone marrow but had lower numbers of these monocytes in the circulating blood compared with control littermates (Fig. 5a and **Supplementary Fig. 13**), suggesting that these mice have impaired monocyte mobilization. *Tnfrsf13c*$^{-/-}$ mice also had lower concentrations of circulating Ccl7 compared to control mice (Fig. 5b). Notably, Baff-r deficiency improved heart function after myocardial infarction, as shown by a significantly higher fractional shortening in *Tnfrsf13c*$^{-/-}$ mice compared with *Tnfrsf13c*$^{+/-}$ littermates (Fig. 5c), despite having no effect on infarct size (**Supplementary Fig. 13**). To further substantiate the role of Baff in this context, we treated a group of WT mice with a Baff-specific monoclonal antibody (Online Methods). We found that Baff neutralization led to significant depletion of circulating B lymphocytes (Fig. 5d), which was associated with impaired Ly6C^{hi} monocyte mobilization (Fig. 5e and **Supplementary Fig. 13**) and improved cardiac function (Fig. 5f).

Blood levels of CCL7 and BAFF and cardiovascular outcome

Finally, we addressed the relevance of these findings to the human disease by assessing the relationship between circulating CCL7 or BAFF concentrations and clinical outcomes in a cohort of 1,000 patients admitted for acute myocardial infarction. The patients' characteristics are given in **Supplementary Tables 1 and 2**. We found that patients with detectable circulating concentrations of CCL7 at the time of admission were at substantially higher risk of death and recurrent myocardial infarction after 2 years of follow-up compared to patients with no detectable CCL7, even after adjustment for several multivariable risk factors (see Online Methods) (hazard ratio = 1.54, 95% confidence interval = 1.07–2.43, P = 0.02) (Fig. 6a). Similarly, the risk of death and recurrent myocardial infarction was associated with increasing tertiles of circulating BAFF concentrations at admission. The hazard ratio of death and recurrent myocardial infarction in the second and third tertiles of BAFF were 1.65 (1.05–2.58) and 3.14 (2.09–4.73), respectively, compared with the lowest tertile (P < 0.0001). The association remained significant in a fully adjusted model (Fig. 6b).

DISCUSSION

B lymphocytes have crucial nonredundant roles mediating both innate and adaptive immune responses through both antibody-dependent and antibody-independent mechanisms. Recent studies have identified new roles for B lymphocytes in the early innate immune response during acute infection[30,31], where B lymphocytes were required to mount an efficient and protective inflammatory response. However, the contribution of B lymphocytes to the inflammatory response secondary to other forms of acute injury, particularly post-ischemic injury, is still poorly defined. Our results uncover a key role for B cell–dependent Ccl7 production in the pathogenic response to acute ischemic injury. The precise B cell subset

involved in this setting remains to be examined in more detail. However, our results indicate that this pathogenic effect of B cells depends in part on Baff-r signaling.

Previous studies did not find a role for B cell responses in post-ischemic stroke injury, as μMT mice showed no difference in infarct size or neurological deficit when compared with WT mice[32]. Other studies addressed the role of B lymphocytes in response to ischemia–reperfusion injury in the kidney. However, very divergent results have been obtained by different groups using B cell–deficient μMT mice in this setting, with studies showing either protection[33,34] or aggravation[12] of ischemia–reperfusion injury. Effects seen in μMT mice should be interpreted with caution given the wide range of immune abnormalities in these mice, as both innate and adaptive B lymphocytes, with potentially divergent functions, are absent. A previous study showed that intramyocar-dial injection of bone marrow–derived B cells after acute myocardial infarction in rats improves the recovery of myocardial function[35]. However, there are major differences between that study and our current work. In the previous study, the injected bone marrow–derived B lymphocytes were mostly immature B cells, which are known to be resistant to CD20 mAb–mediated B cell depletion. In addition, the mechanisms of protection afforded by immature B lymphocyte injection were unclear, and the investigators did not assess the role of endogenous B lymphocytes.

We and others have shown that Baff-r deficiency or CD20 mAb–induced B cell depletion holds promise in the context of cardiovascular disease and reduces the development of atherosclerotic lesions in several experimental models[25,36–38]. Our present data show that depletion of mature B lymphocytes after CD20 mAb injection during the acute phase of myocardial infarction leads to marked improvement in both post-ischemic ventricular remodeling and myocardial function. We obtained similar results with Baff-r deficient mice or a neutralizing Baff-specific antibody. CD20 mAb treatment also led to a substantial reduction of infarct size, which was not observed after blockade of Baff signaling. It should be noted that Baff-r is also expressed on non-B cells and may activate multiple cell types with opposite and confounding effects on cardiac homeostasis. In addition, B cell depletion in mice treated with Baff-specific antibody was delayed, so that a second antibody injection at day 1 was necessary to obtain a substantial depletion. In contrast, B cells quickly disappeared from the blood in CD20 mAb–treated mice after a single antibody injection.

Future work should address the mechanisms responsible for B cell activation after acute ischemic injury and the pathways that drive B cell–dependent Ccl7 production. For example, endogenous Toll-like receptor ligands might accumulate after necrosis and could lead to B cell activation. Notably, splenic B cells of *Myd88*$^{-/-}$; *Trif*$^{-/-}$ mice, which are unable to respond to TLR stimulation, produced substantially less Ccl7 than did splenic B cells of WT mice. Whether this effect is related to selective Myd88 or Trif (or both Myd88 and Trif) signaling in B cells and whether this effect can directly affect systemic Ccl7 concentrations remains to be determined. Moreover, it will be important to address in more detail the contribution of the various B cell and monocyte subsets to post-ischemic injury. The substantial reduction of the number of Ly6C^{lo} monocytes in blood after B cell depletion or blockade of Baff signaling might be in part related to reduced Ccl7 signaling[28] or may suggest the involvement of additional chemokine pathways, such as the Cx3cr1 pathway. However, we found no difference in Cx3cl1 production between CD20-depleted and control

mice (unpublished results, Y.Z.). Finally, pilot data suggest that Cxcl13 may be induced after myocardial infarction (unpublished results, Y.Z.) and might therefore have a role in B cell recruitment into the ischemic heart.

In summary, these studies delineate a key contributory role for systemic B cells during the immune responses that lead to tissue damage after acute myocardial infarction. Neutrophils, monocyte subsets, NK cells and T cells enter the site of injury. The release of inflammatory mediators and tissue antigens seems to result in the rapid activation of B cells systemically, which leads to B cell production of Ccl7, in part through a Myd88 and/or Trif-dependent pathway. B cells are also secondarily recruited to the ischemic heart as a component of the inflammatory response. B cell–derived Ccl7 probably acts synergistically with Ccl7 produced from other cellular sources to increase serum chemokine concentrations, facilitating the mobilization of monocytes from the bone marrow and resulting in enhanced monocyte entry into sites of tissue damage. B cell depletion reduces Ccl7 production and the magnitude of $7/4^{hi}$ monocyte recruitment and macrophage accumulation into post-ischemic tissues. Because B cells are well known to promote proinflammatory innate and adaptive immune responses[39], their systemic depletion is likely to further reduce T cell–, macrophage- and neutrophil-induced tissue damage by reducing the systemic amplification of the inflammatory response after myocardial infarction. As a consequence, B cell depletion has a profound impact on post-ischemic injury, as shown here. B cell depletion substantially limits myocardial inflammation, reduces infarct size and improves myocardial function. The positive association of circulating concentrations of BAFF and CCL7 with adverse outcomes in patients with acute myocardial infarction strongly supports the clinical relevance of these findings to the human disease.

In our experiments, CD20 mAb and Baff-specific mAb were administered 1 h after the induction of myocardial infarction, mimicking the clinical setting in which a therapeutic agent is administered in the first hours after the onset of clinical signs of acute ischemic injury. Thus, we believe that our study sets the stage for the testing of available humanized B cell–depleting antibodies during the acute phase of myocardial infarction with the aim of limiting myocardial necrosis and inflammation and improving the recovery of heart function. In addition, we anticipate that therapies targeting pathways that control mature B lymphocytes, such as Baff and Ccl7 pathways, should be of interest in the setting of acute ischemic injury.

ONLINE METHODS

Myocardial infarction

All mice were on a C57BL/6J background. C57BL/6 (Janvier), *Ccl7*$^{-/-}$ (ref. 28), *Tnfrsf13c*$^{-/-}$ (The Jackson Laboratory), *Rag1*$^{-/-}$ and CD45.1 mice (Janvier) and *Myd88*$^{-/-}$; *Trif*$^{-/-}$ mice (provided by B. Ryffel[40]) were studied at 8 weeks of age. *Tnfrsf13c*$^{+/-}$ mice were generated by crossing *Tnfrsf13c*$^{-/-}$ mice with C57BL/6J mice. Myocardial infarction was induced by left coronary ligation[41]. Mice were anesthetized using ketamine (100 mg per kg body weight) and xylazine (10 mg per kg body weight) via intraperitoneal injection (i.p.) and then intubated and ventilated with air using a small-animal respirator. The chest wall was shaved and a thoracotomy was performed in the fourth left intercostal space. The left

ventricle was visualized, the pericardial sac was then removed, and the left anterior descending artery was permanently ligated using a 7/0 monofilament suture (Peters surgical, France) at the site of its emergence from under the left atrium. Significant color changes at the ischemic area were considered indicative of successful coronary occlusion. The thoracotomy was closed with 6/0 monofilament sutures. The same procedure was performed for sham-operated control mice except that the ligature was left untied. The endotracheal tube was removed once spontaneous respiration resumed, and mice were placed on a warm pad maintained at 37 °C until they were completely awake. One hour after myocardial infarction induction, mice were treated i.p. with a previously validated mouse monoclonal anti-CD20 antibody (200 μg per mouse[24,25], with an anti-Baff antibody (clone 10F4, kindly provided by Human Genome Sciences 100 μg per mouse, repeated at day 1 after myocardial infarction)[42] or with PBS. In leukocyte recruitment experiments, CD20 mAb–treated mice or the PBS-treated group received 15×10^6 $CD45.1^+$ bone marrow–derived mononuclear cells 4 h after myocardial infarction. Bone marrow cells were obtained by flushing tibiae and femora of $CD45.1^+$ donor mice. Low-density bone marrow–derived mononuclear cells were then isolated by density gradient centrifugation with Ficoll (Histopaque-1083, Sigma-Aldrich). In other sets of experiments, 7 d before myocardial infarction induction, *Rag1*$^{-/-}$ mice received either 2×10^7 WT splenocytes, 1.2×10^7 B cell–depleted splenocytes recovered from CD20 mAb–treated WT mice (one injection of 200 μg per mouse, mice were used 3 d after), or B cell–depleted splenocytes resupplemented with 8×10^6 WT B lymphocytes or with 8×10^6 *Ccl7*$^{-/-}$ B lymphocytes Procedures for isolation of splenocytes and B lymphocytes are described below. In additional experiments, we generated a B cell–restricted *Ccl7*-deficient mouse model by reconstituting lethally irradiated WT mice with a mixture of μMT and *Ccl7*$^{-/-}$ bone marrow as previously described[31,37]. In this case, all reconstituted B cells originate from *Ccl7*$^{-/-}$ bone marrow and are therefore completely deficient in Ccl7. The control group received a mixture of μMT and *Ccl7*$^{+/+}$ bone marrow. Mice were allowed to recover for 5 weeks. Experiments were conducted according to the French veterinary guidelines and those formulated by the European Community for experimental animal use and were approved by the Institut National de la Santé et de la Recherche Médicale.

Echocardiographic measurements

Transthoracic echocardiography was performed 14 d after surgery using an echocardiograph (ACUSON S3000 ultrasound, Siemens AG, Erlangen, Germany) equipped with a 14-MHz linear transducer (1415SP). The investigator was blinded to group assignment. Mice were anesthetized by isoflurane inhalation. Two-dimensional parasternal long-axis views of the left ventricle were obtained for guided M-mode measurements of the LV internal diameter at end diastole (LVDD) and end systole (LVDS), as well as the interventricular septal wall thickness and posterior wall thickness. Percentage fractional shortening (%FS) was calculated by the following formula: $\%\mathrm{FS} = [(\mathrm{LVDD} - \mathrm{LVDS})/\mathrm{LVDD}] \times 100$.

Histopathological analysis

Cardiac healing after myocardial infarction was assessed at day 14. Hearts were excised, rinsed in PBS and frozen in liquid nitrogen. Hearts were cut by a cryostat (CM 3050S, Leica) into 7-μm-thick sections. Masson's trichrome and Sirius red stainings were

performed for infarct size and myocardial fibrosis evaluation. Infarct size (in %) was calculated as total infarct circumference divided by total LV circumference. The collagen volume fraction was calculated as the ratio of the total area of interstitial fibrosis to the myocyte area in the entire visual field of the section. B lymphocyte immunostaining was performed according to an indirect immunoperoxidase method using a rat biotin conjugated anti-CD45R/B220 antibody (RA3-6B2, Southern Biotechnology) at a dilution of 1:50 and the AEC substrate chromogen kit (K3464, Dako). Endothelial cells within capillaries were visualized after BS-1 lectin staining (1:100, FITC-conjugated *Griffonia simplicifolia*, Sigma-Aldrich) and arterioles using a rabbit anti–mouse α-actin smooth muscle antibody (1:100, AC-40, Sigma-Aldrich) followed by staining with a donkey DyLight649– anti-rabbit IgG (1/100, 95543, Jackson ImmunoResearch).

Cells

Mice were killed at 12 h and on days 1, 3, 5, 7 and 14 after myocardial infarction (n = 5–10 mice per time point). Peripheral blood was drawn via inferior vena cava puncture with heparin solution. Whole blood was lysed after immunofluorescence staining using the BD FACS lysing solution (BD Biosciences), and total blood leukocyte numbers were determined using trypan blue. Bone marrow cells were drawn from femur and tibia and filtered through a 40-μm nylon mesh (BD Biosciences). Spleens were collected, minced with fine scissors and filtered through a 40-μm nylon mesh (BD Biosciences). For both splenocytes and bone marrow–derived cells, the cell suspension was centrifuged at 400g for 10 min at 4 °C. Red blood cells were lysed using red blood cell lysing buffer (Sigma-Aldrich) and splenocytes and bone marrow cells were washed with PBS supplemented with 3% (vol/vol) FBS. Hearts were collected, minced with fine scissors and placed into a cocktail of collagenase I (450 U ml^{-1}), collagenase XI (125 U ml^{-1}), DNase I (60 U ml^{-1}), and hyaluronidase (60 U ml^{-1}) (Sigma-Aldrich) and shaken at 37 °C for 1 h. Cells were then triturated through a nylon mesh (40 μm) and centrifuged (10 min, 400g, 4 °C). Mononuclear cells were purified by density centrifugation using Ficoll (Histopaque-1083, Sigma-Aldrich) (25 min, 400g, room temperature). The resulting cell suspensions were washed using PBS, and total leukocyte numbers were determined.

Cell purification, culture and transmigration assay

B cells were isolated from C57BL/6J spleens using a B cell isolation kit (Miltenyi Biotec) according to the manufacturer's protocol. B cells were stimulated for 48 h with 10 μg ml^{-1} of anti–mouse IgM (Jackson ImmunoResearch) and 2.5 μg ml^{-1} of anti–mouse CD40 (clone HM40-3, BioLegend). Monocytes were isolated from bone marrow, as follows. The fraction of monocytes in the bone marrow was enriched by neutrophil depletion using autoMACS columns (Miltenyi Biotec) and anti-Ly6G magnetic beads (Miltenyi Biotec). $7/4^{hi}$ monocytes (7/4 staining is equivalent to Ly6C staining[43]) were then sorted on a FACSAria (BD Biosciences). *In vitro* monocyte transmigration assays were performed over cell culture inserts (Millicell-PCF, Millipore) with porous polycarbonate filters (8 μm pore size) in 24-well plates. Inserts were coated with rat-tail type I collagen (BD Biosciences) (60 μg ml^{-1}) for 30 min at 37 °C and then blocked with 3% (wt/vol) BSA in PBS for 1 h at 37 °C. 2×10^6 of B lymphocytes in 300 μL of RPMI-10% (vol/vol) FBS were added to the lower compartment, and 9×10^4 of $7/4^{hi}$ monocytes in 200 μL of the same medium was added to

the upper compartment. No cells could be counted when B cells were cultured in the absence of monocytes in the upper compartment, indicating no B cell contamination. Ccl7-specific neutralizing antibody (2 μg ml^{-1}, AF-456-NA, R&D Systems) or 1 μg ml^{-1} of Ccl2-neutralizing antibody (AF-479-NA, R&D Systems) were added to the lower compartment at the start of the migration assay. Monocytes were allowed to migrate for 4 h at 37 °C. The filters were then washed with PBS and fixed in 1% paraformaldehyde. The upper surfaces of the filters were scraped with cotton swabs to remove nonmigrating cells. The filters were then stained with DAPI (Sigma-Aldrich). Migrating cells attached to the lower surface of the filters were visualized under an Axioimager Z1 microscope (Zeiss). Each experiment was performed in triplicate.

Flow cytometry

The following antibodies were used: FITC-conjugated anti-CD11b (M1/70, BD Pharmingen), phycoerythrin (PE)-conjugated anti-Ly6G (1A8, BD Pharmingen), PE-conjugated anti-NK-1.1 (PK 136, BD Pharmingen), allophycocyanin (APC)-conjugated anti-Ly-6B.2 (clone 7/4, AbD Serotec), APC-conjugated anti-CD3e (17A2, eBioscience), FITC-conjugated anti-CD4 (RM 4-5, eBioscience), PercP-conjugated anti-CD8a (53-6.7, BD Pharmingen), PE-conjugated anti-CD45R/B220 (RA3-6B2, eBioscience), APC-conjugated anti-IgM (II/41, eBioscience), PE-Cy7–conjugated anti-CD11c (N418, eBioscience), APC-conjugated anti-CD19 (1D3, BD Pharmingen), V450- conjugated anti-IgD (11-26C.2A, BD Horizon), PE-Cy7-conjugated anti-CD21 (7E9, Biolegend), PE-conjugated anti-CD23 (B3B4, BD Pharmingen), biotinylated anti-Ccl7 (500-P116GBt, PeproTech), and APC-conjugated anti-CD45.1 (A20, BD Pharmingen). All antibodies were used at a dilution of 1:100 except for APC-conjugated anti-Ly-6B.2, which was used at 1:20. Monocytes were identified as $CD11b^{hi}Ly6G^{-}7/4^{hi/lo}$. Neutrophils were identified as $CD11b^{+}Ly6G^{hi}7/4^{hi}$. Macrophages and dendritic cells were identified as $CD11c^{hi}$. Natural killer cells were identified as $CD11b^{+}Ly6G^{-}7/4^{-}NK1.1^{+}$. Mature B lymphocytes were identified as $B220^{hi}IgM^{hi}$. The total number of cells was then normalized to heart weight. Cells were analyzed using a flow cytometer (LSR II, BD Biosciences).

Antibody measurements

Circulating IgM, IgG1, and IgG2c levels were measured in serum of treated mice using a chemiluminescence-based sandwich ELISA and matched pairs of specific antibodies for capture and detection. The following antibodies were paired with appropriate detecting antibodies: goat anti-mouse IgM (Sigma-Aldrich; M8644) with alkaline phosphatase (AP)-labeled goat anti-mouse IgM (Sigma-Aldrich; A 9688); rat anti-mouse IgG1 (Biolegend; 406602) with biotinylated rat anti-mouse IgG1 (BD; 553441); and goat anti-mouse IgG2c (AbD Serotec; STAR135) with biotinylated goat anti-mouse IgG2c (Jackson ImmunoResearch; 115-065-208). An extra incubation step with AP-labeled NeutrAvidin (Pierce) was performed in assays in which biotinylated detection antibodies were used. All ELISA assays were developed using LumiPhos Plus (Lumigen). Purified immunoglobulin isotypes used for standardization were purchased from Biolegend or Southern Biotech. The detection limit for IgM Abs was ~0.8 ng ml^{-1}, for IgG1 ~0.15 ng ml^{-1} and for IgG2c ~7pg ml^{-1}. Serum was used at dilutions of 1:10,000 for total IgM, 1:450,000 for total IgG1 and 1:150,000 for total IgG2c.

Quantitative real-time PCR

Quantitative real-time PCR was performed on a Step-One Plus (Applied Biosystems). GAPDH was used to normalize gene expression. The following primer sequences were used: forward 5′-CGT-CCCGTAGACAAAATGGTGAA-3′, reverse 5′-GCCGTGAGTGGAGTCATACTGGAA-CA-3′; IL-1β: forward 5′-GAAGAGCCCATCCTCTGTGA-3′, reverse 5′-GGGTGTGCCGTCTTTCATTA-3′; TNF-α: forward 5′-GATGGGGGGC TTCCAGAACT-3′, reverse 5′-GATGGGGGGCTTCCAGAACT-3′; IL-18: forward 5′-AGTGAACCCCAGACCAGACTGA-3′, reverse 5′-CCCTCCCCACCTAACTTTGATGTA-3′; TGF-β: forward 5′-CGGAGAGCCCTGGATACCAACTA-3′, reverse 5′-GCCGCACACAGCAGTTCTTCTCT-3′.

Chemokine concentrations

Plasma and/or heart concentrations of Ccl2, Ccl12, Cxcl13 and Ccl7 were measured using Quantikine ELISA Kits (R&D Systems) according to the manufacturer's instructions.

Population of patients with acute myocardial infarction

The demographics and methodology of the French Registry of Acute ST-Elevation and Non– ST-Elevation Myocardial Infarction (FAST-MI) have been described in detail in previous publications[44]. Briefly, all patients were included in the registry if they were ≥18 years of age and had elevated serum markers of myocardial necrosis higher than twice the upper limit of normal for creatine kinase, creatine kinase-MB or elevated troponins, and either symptoms compatible with acute myocardial infarction and/or electrocardiographic changes on at least two contiguous leads with pathologic Q waves (≥0.04 s) and/or persisting ST elevation or depression > 0.1 mV. The time from symptom onset to intensive care unit admission had to be <48 h. Patients were managed according to usual practice; treatment was not affected by participation in the registry. Of the 374 centers in France that treated patients with acute myocardial infarction at the time during which patients were recruited for this study, 223 (60%) participated in the registry. Among these, 100 centers recruited 1,029 patients who contributed to a serum bank. For the present study, 1,000 samples were available for CCL7 measurement and 959 samples were available for BAFF measurement. Written informed consent was provided by each patient. The baseline (at the time of admission for acute myocardial infarction) characteristics of the patients who contributed samples used for CCL7 and BAFF measurements were comparable to those of the overall population of the registry. More than 99% of patients were Caucasians. Follow-up data was collected through contacts with the patients' physicians, the patients themselves, their families or the registry offices of their birthplaces. Follow-up at one year was >99%. The study was reviewed and approved by the Committee for the Protection of Human Subjects in Biomedical Research of Saint Antoine University Hospital, and the data file was declared to the Commission Nationale Informatique et Liberté. Human CCL7 analysis was carried out using the Bioplex Pro magnetic technology (Bio-Plex Pro Human Cytokine CCL7 Set 171-B6012M, Bio-Rad), following the manufacturer's instructions. Frozen (−80 °C) EDTA plasma samples from each patient were all analyzed on the same day. Samples

were thawed and spun at 2,500*g* for 15 min at room temperature before use, and particle-clear plasma was used at 1:4 dilution. Data were acquired on 50 beads per patient and analyzed following a 1:4 serial dilution standard curve (the concentrations in the linear range of the assay were 0.33–3,472 pg ml^{-1}) using the Bio-Plex Manager 6.1 Software and 5PL logistic regression (FitProb. = 0.0000, ResVar. = 7.7585). BAFF was measured using Quantikine human Baff Immunoassay (ref. SBLYS0, R&D Systems) according to the manufacturer's instructions.

Statistical analyses

For experimental animal studies, results are expressed as mean ± s.e.m. Kruskal-Wallis was used to compare each parameter. *Post hoc* Mann-Whitney *U* tests with Bonferroni's correction were then performed. Statistical analysis of FAST-MI registry data was conducted as follows. An outcome event was defined as all-cause death or nonfatal myocardial infarction during the 1-year follow-up period. The primary endpoint was defined as a composite of all-cause death and nonfatal myocardial infarction and was adjudicated by a committee whose members were unaware of patients' medications and blood measurements. Continuous variables are described as mean ± s.d. and categorical variables as frequencies or percentages. Baseline demographic and clinical characteristics, treatment factors and therapeutic management during hospitalization were compared among patients with or without detectable circulating CCL7 levels using chi-square or Fisher' s exact tests for discrete variables and by unpaired *t*-tests or Wilcoxon sign-rank tests for continuous variables. Survival curves according to detectable or undetectable CCL7 levels are estimated using the Kaplan-Meier estimator. We used a multivariable Cox proportional-hazards model to assess the independent prognostic value of variables with the primary endpoint during the 1-year follow-up period. The multivariable model comprised sex, age, previous or current smoking, family history of coronary disease, history of hypertension, previous myocardial infarction, heart failure, renal failure, diabetes, heart rate at admission, Killip class, left ventricular ejection fraction, hospital management (including reperfusion therapy, statins, beta blockers, clopidogrel, diuretics, digitalis, heparin), troponin I and log CRP levels. Results are expressed as hazard ratios for Cox models with 95% confidence intervals (CIs). All statistical tests were two-sided and performed using SAS software version 9.1.

Acknowledgments

This work was supported by INSERM, the British Heart Foundation (Z.M.), the European Research Council (Z.M.), Fondation Coeur et Recherche (Z.M., T.S. and N.D.), Fondation pour la Recherche Médicale (J.-S.S.), European Union Seven Framework programme TOLERAGE (Z.M.), Fondation Leducq Transatlantic Network (C.J.B., D.T., A.T., J.-S.S. and Z.M.), US National Institutes of Health grants AI56363 and AI057157, and a grant from The Lymphoma Research Foundation (T.F.T.). We are indebted to M.O. Kozma, L. Baker and J. Harrison for excellent technical assistance. The Baff-specific antibody was a kind gift from Human Genome Sciences. *Myd88*$^{-/-}$; *Trif*$^{-/-}$ mice were provided by B. Ryffel (Unité Mixte de Recherche 7355, Orléans, France). Y.Z. is a recipient of fellowships from Fondation pour la Recherche Médicale and from Journées de Biologie Clinique. We thank the physicians who cared for the patients at the participating institutions, the International Clinical Trials Association Contract Research Organization (Fontaine-lès-Dijon, France), E. Drouet and the Clinical Research Assistant team of Unité de Recherche Clinique de l'Est Parisien (Assistance Publique–Hôpitaux de Paris and UPMC Paris 06), B. Pace, V. Bataille and G. Mulak (French Society of Cardiology) for their assistance in designing the electronic case-record form and data management during the follow-up period.

References

1. White HD, Chew DP. Acute myocardial infarction. Lancet. 2008; 372:570–584. [PubMed: 18707987]
2. Jessup M, Brozena S. Heart failure. N Engl J Med. 2003; 348:2007–2018. [PubMed: 12748317]
3. McMurray JJ, Pfeffer MA. Heart failure. Lancet. 2005; 365:1877–1889. [PubMed: 15924986]
4. Shah AM, Mann DL. In search of new therapeutic targets and strategies for heart failure: recent advances in basic science. Lancet. 2011; 378:704–712. [PubMed: 21856484]
5. Nabel EG, Braunwald E. A tale of coronary artery disease and myocardial infarction. N Engl J Med. 2012; 366:54–63. [PubMed: 22216842]
6. Yellon DM, Hausenloy DJ. Myocardial reperfusion injury. N Engl J Med. 2007; 357:1121–1135. [PubMed: 17855673]
7. Taqueti VR, Mitchell RN, Lichtman AH. Protecting the pump: controlling myocardial inflammatory responses. Annu Rev Physiol. 2006; 68:67–95. [PubMed: 16460267]
8. Zhang M, et al. Identification of a specific self-reactive IgM antibody that initiates intestinal ischemia/reperfusion injury. Proc Natl Acad Sci USA. 2004; 101:3886–3891. [PubMed: 14999103]
9. Zhang M, et al. Identification of the target self-antigens in reperfusion injury. J Exp Med. 2006; 203:141–152. [PubMed: 16390934]
10. Zhang M, et al. Activation of the lectin pathway by natural IgM in a model of ischemia/reperfusion injury. J Immunol. 2006; 177:4727–4734. [PubMed: 16982912]
11. Haas MS, et al. Blockade of self-reactive IgM significantly reduces injury in a murine model of acute myocardial infarction. Cardiovasc Res. 2010; 87:618–627. [PubMed: 20462867]
12. Renner B, et al. B cell subsets contribute to renal injury and renal protection after ischemia/reperfusion. J Immunol. 2010; 185:4393–4400. [PubMed: 20810984]
13. Pepys MB, et al. Targeting C-reactive protein for the treatment of cardiovascular disease. Nature. 2006; 440:1217–1221. [PubMed: 16642000]
14. Salio M, et al. Cardioprotective function of the long pentraxin PTX3 in acute myocardial infarction. Circulation. 2008; 117:1055–1064. [PubMed: 18268142]
15. Granger DN, Korthuis RJ. Physiologic mechanisms of postischemic tissue injury. Annu Rev Physiol. 1995; 57:311–332. [PubMed: 7778871]
16. Vinten-Johansen J. Involvement of neutrophils in the pathogenesis of lethal myocardial reperfusion injury. Cardiovasc Res. 2004; 61:481–497. [PubMed: 14962479]
17. Nahrendorf M, et al. The healing myocardium sequentially mobilizes two monocyte subsets with divergent and complementary functions. J Exp Med. 2007; 204:3037–3047. [PubMed: 18025128]
18. Leuschner F, et al. Rapid monocyte kinetics in acute myocardial infarction are sustained by extramedullary monocytopoiesis. J Exp Med. 2012; 209:123–137. [PubMed: 22213805]
19. Mahaffey KW, et al. Effect of pexelizumab, an anti-C5 complement antibody, as adjunctive therapy to fibrinolysis in acute myocardial infarction: the COMPlement inhibition in myocardial infarction treated with thromboLYtics (COMPLY) trial. Circulation. 2003; 108:1176–1183. [PubMed: 12925455]
20. Granger CB, et al. Pexelizumab, an anti-C5 complement antibody, as adjunctive therapy to primary percutaneous coronary intervention in acute myocardial infarction: the COMplement inhibition in Myocardial infarction treated with Angioplasty (COMMA) trial. Circulation. 2003; 108:1184–1190. [PubMed: 12925454]
21. Armstrong PW, et al. Pexelizumab for acute ST-elevation myocardial infarction in patients undergoing primary percutaneous coronary intervention: a randomized controlled trial. J Am Med Assoc. 2007; 297:43–51.
22. Eikelboom JW, O'Donnell M. Pexelizumab does not "complement" percutaneous coronary intervention in patients with ST-elevation myocardial infarction. J Am Med Assoc. 2007; 297:91–92.
23. Martin F, Chan AC. B cell immunobiology in disease: evolving concepts from the clinic. Annu Rev Immunol. 2006; 24:467–496. [PubMed: 16551256]

24. Uchida J, et al. Mouse CD20 expression and function. Int Immunol. 2004; 16:119–129. [PubMed: 14688067]
25. Ait-Oufella H, et al. B cell depletion reduces the development of atherosclerosis in mice. J Exp Med. 2010; 207:1579–1587. [PubMed: 20603314]
26. Hamaguchi Y, et al. The peritoneal cavity provides a protective niche for B1 and conventional B lymphocytes during anti-CD20 immunotherapy in mice. J Immunol. 2005; 174:4389–4399. [PubMed: 15778404]
27. Busche MN, Pavlov V, Takahashi K, Stahl GL. Myocardial ischemia and reperfusion injury is dependent on both IgM and mannose-binding lectin. Am J Physiol Heart Circ Physiol. 2009; 297:H1853–H1859. [PubMed: 19749170]
28. Tsou CL, et al. Critical roles for CCR2 and MCP-3 in monocyte mobilization from bone marrow and recruitment to inflammatory sites. J Clin Invest. 2007; 117:902–909. [PubMed: 17364026]
29. Mackay F, Schneider P. Cracking the BAFF code. Nat Rev Immunol. 2009; 9:491–502. [PubMed: 19521398]
30. Kelly-Scumpia KM, et al. B cells enhance early innate immune responses during bacterial sepsis. J Exp Med. 2011; 208:1673–1682. [PubMed: 21746813]
31. Rauch PJ, et al. Innate response activator B cells protect against microbial sepsis. Science. 2012; 335:597–601. [PubMed: 22245738]
32. Yilmaz G, Arumugam TV, Stokes KY, Granger DN. Role of T lymphocytes and interferon-γ in ischemic stroke. Circulation. 2006; 113:2105–2112. [PubMed: 16636173]
33. Burne-Taney MJ, et al. B cell deficiency confers protection from renal ischemia reperfusion injury. J Immunol. 2003; 171:3210–3215. [PubMed: 12960350]
34. Jang HR, et al. B cells limit repair after ischemic acute kidney injury. J Am Soc Nephrol. 2010; 21:654–665. [PubMed: 20203156]
35. Goodchild TT, et al. Bone marrow–derived B cells preserve ventricular function after acute myocardial infarction. JACC Cardiovasc Interv. 2009; 2:1005–1016. [PubMed: 19850263]
36. Kyaw T, et al. Conventional B2 B cell depletion ameliorates whereas its adoptive transfer aggravates atherosclerosis. J Immunol. 2010; 185:4410–4419. [PubMed: 20817865]
37. Sage AP, et al. BAFF receptor deficiency reduces the development of atherosclerosis in mice—brief report. Arterioscler Thromb Vasc Biol. 2012; 32:1573–1576. [PubMed: 22426131]
38. Kyaw T, et al. Depletion of B2 but not B1a B cells in BAFF receptor–deficient ApoE mice attenuates atherosclerosis by potently ameliorating arterial inflammation. PLoS ONE. 2012; 7:e29371. [PubMed: 22238605]
39. Yanaba K, et al. B-lymphocyte contributions to human autoimmune disease. Immunol Rev. 2008; 223:284–299. [PubMed: 18613843]
40. Togbe D, et al. Nonredundant roles of TIRAP and MyD88 in airway response to endotoxin, independent of TRIF, IL-1 and IL-18 pathways. Lab Invest. 2006; 86:1126–1135. [PubMed: 16983331]
41. Kumar D, et al. Distinct mouse coronary anatomy and myocardial infarction consequent to ligation. Coron Artery Dis. 2005; 16:41–44. [PubMed: 15654199]
42. Scholz JL, et al. BLyS inhibition eliminates primary B cells but leaves natural and acquired humoral immunity intact. Proc Natl Acad Sci USA. 2008; 105:15517–15522. [PubMed: 18832171]
43. Cochain C, et al. Regulation of monocyte subset systemic levels by distinct chemokine receptors controls post-ischaemic neovascularization. Cardiovasc Res. 2010; 88:186–195. [PubMed: 20501509]
44. Simon T, et al. Genetic determinants of response to clopidogrel and cardiovascular events. N Engl J Med. 2009; 360:363–375. [PubMed: 19106083]

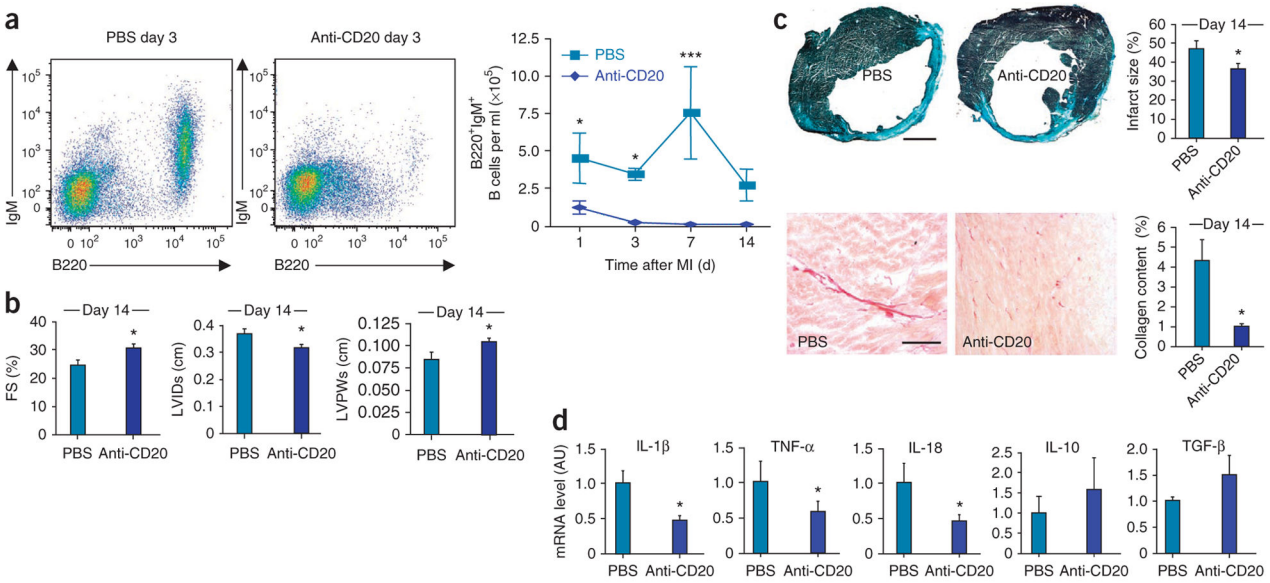

Figure 1.

The B cell–depleting CD20 mAb reduces infarct size, improves heart function and limits myocardial inflammation. (**a**) Representative examples (left) and quantitative analysis (right) of B220^{hi} IgM^{+} B cell staining in the blood of C57BL/6J mice treated with or without the CD20 mAb (anti-CD20) (n = 12–15 mice per group); ***P < 0.001. MI, myocardial infarction. (**b**) Echocardiographic analysis after anti-CD20 therapy. Left ventricular fractional shortening (FS), left ventricular internal diameter at end systole (LVIDs) and left ventricular posterior wall thickness at end systole (LVPWs) were measured at day 14 after myocardial infarction; *P < 0.05. (**c**) Representative photomicrographs (left) and quantitative analysis (right) of infarct size and myocardial fibrosis evaluation evaluated by Masson trichrome (top) and Sirius red (bottom) staining, respectively, measured at day 14 after myocardial infarction. Data are representative of 10–14 mice per group in three independent experiments. Scale bars: top, 1 mm; bottom,100 μm. (**d**) mRNA levels of the proinflammatory cytokines IL-1β, TNF-α and IL-18 and the anti-inflammatory cytokines IL-10 and TGF-β within the injured myocardium on day 14 after myocardial infarction (n = 8–12 mice per group). AU, arbitrary units. Mean values ± s.e.m. are represented. *P < 0.05 versus PBS.

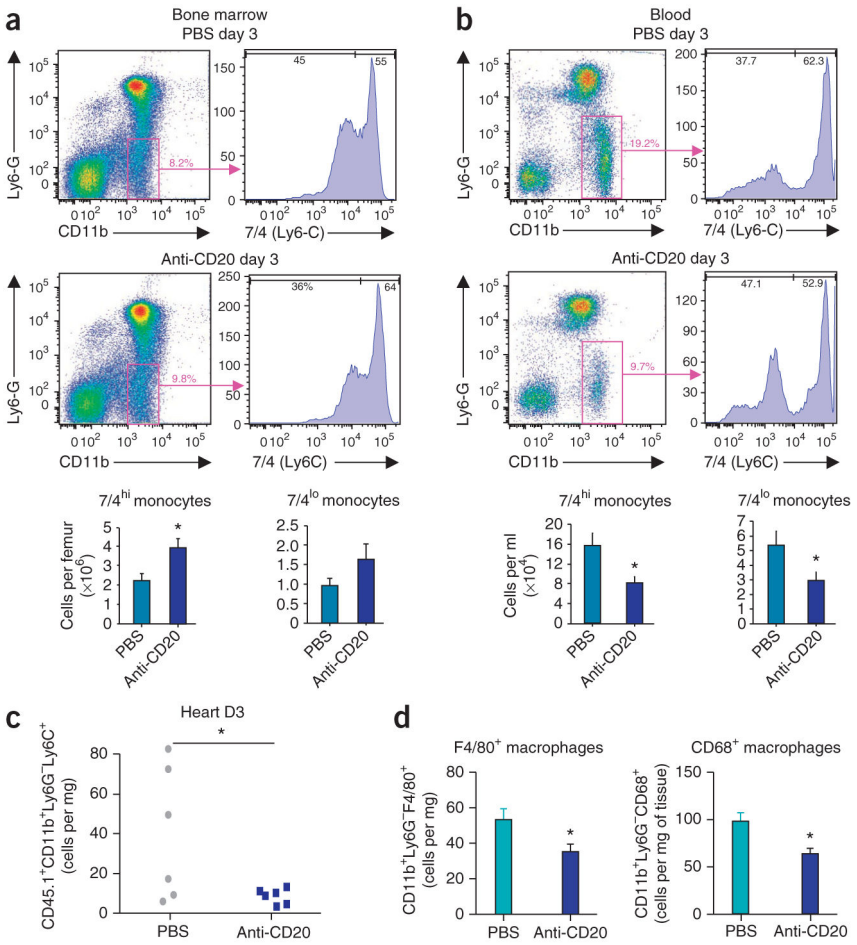

Figure 2.

B lymphocyte depletion impairs monocyte mobilization and recruitment and macrophage accumulation in the injured myocardium. (**a**,**b**) Representative examples of 7/4^{hi} and 7/4^{lo} monocyte staining (top) and quantification of their numbers (bottom) in bone marrow (**a**) and blood (**b**) of B cell–depleted mice compared to controls on day 3 after myocardial infarction (n = 8–15 mice per group). Mean values ± s.e.m. are represented. *P < 0.05 versus PBS. 7/4 (Ly6C) indicates staining with antibody clone 7/4 directed against the Ly-6B.2 alloantigen, whose staining is equivalent to staining with Ly6C. (**c**) Quantitative analysis of the number of CD45.1^{+}CD11b^{+}Ly6G^{-}Ly6C^{+} cells in the cardiac tissue of anti-CD20–treated mice compared to controls on day 3 after myocardial infarction (n = 6 mice per group). Each symbol represents an individual mouse. (**d**) Quantitative analysis of the number of F4/80^{+} and CD68^{+} macrophages within the myocardium on day 5 after myocardial infarction (n = 5 mice per group). Mean values ± s.e.m. are represented. *P < 0.05 versus PBS.

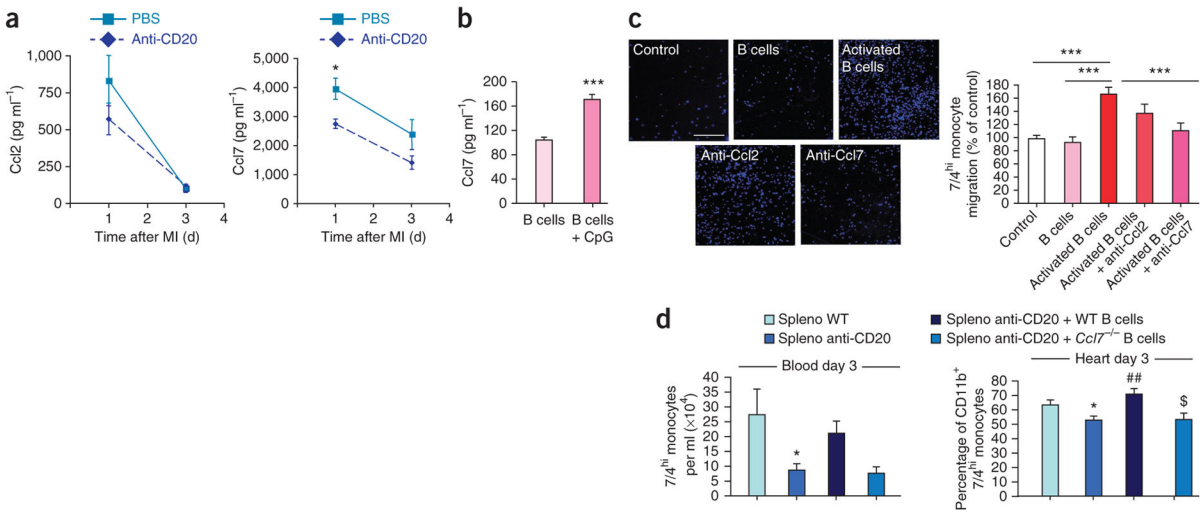

Figure 3.

B lymphocyte depletion significantly lowers Ccl7 concentrations after acute myocardial infarction and triggers Ccl7-dependent monocyte transmigration *in vitro* and *in vivo*. (**a**) Ccl2 and Ccl7 protein concentrations in blood after CD20 mAb or control PBS treatment, 1 and 3 d after myocardial infarction (n = 5–8 mice per group); *P < 0.05 versus PBS. (**b**) Ccl7 concentrations in the supernatant of nonstimulated or CpG-stimulated cultured splenic B cells isolated from WT mice. Data are representative of four independent experiments; each condition was tested in triplicate. Mean values ± s.e.m. are shown. ***P < 0.001 versus untreated B cells. (**c**) Representative photomicrographs (left) and histograms (right) of the transmigration of cultured monocytes in the presence of nonstimulated or activated (using IgM and CD40) B cells with or without neutralizing anti-Ccl2 or anti-Ccl7 antibodies. Data are representative of four independent experiments; each condition was tested in triplicate. Scale bar, 300 μm. Mean values ± s.e.m. are shown. ***P < 0.001 versus control condition without B cells. (**d**) Quantification of the number of 7/4^{hi} monocytes in blood (left) and their percentages in infarcted myocardium (right) of *Rag1*$^{-/-}$ mice injected with WT splenocytes, B cell–depleted splenocytes, or B cell–depleted splenocytes resupplemented with WT or *Ccl7*$^{-/-}$ B cells, 3 d after myocardial infarction. Data are representative of 10–12 mice per group in two independent experiments. Mean values ± s.e.m. are shown. *P < 0.05 versus WT splenocytes; $^{\#\#}P$ < 0.01 versus anti-CD20 splenocytes; $^{\$}P$ < 0.05 versus anti-CD20 splenocytes with WT B cells.

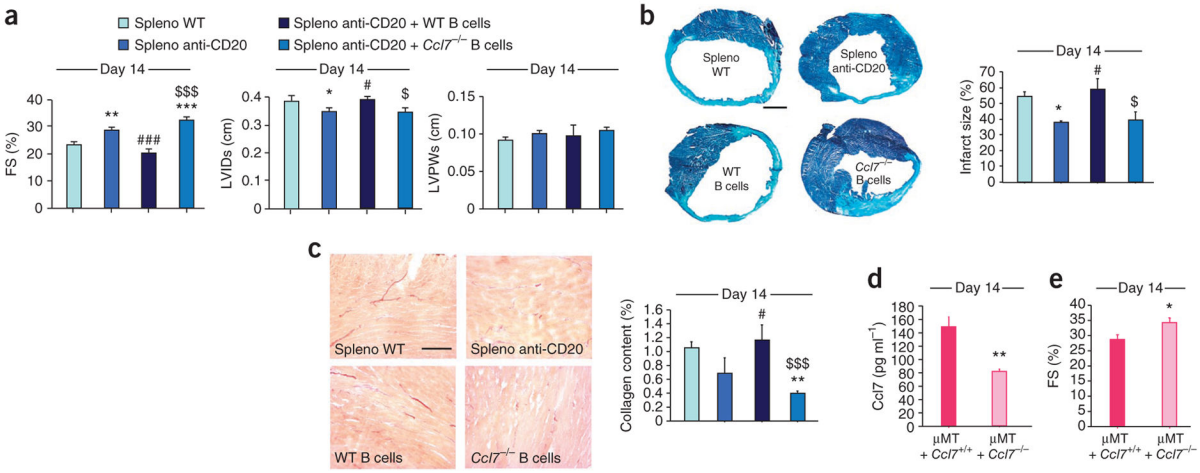

Figure 4.

B lymphocytes trigger adverse ventricular remodeling and alter heart function through the production of Ccl7. (**a**) Echocardiographic analysis 14 d after myocardial infarction. Shown are FS, LVIDs and LVPWs of *Rag1*$^{-/-}$ mice injected with either WT splenocytes, B cell–depleted splenocytes or B cell–depleted splenocytes resupplemented with WT or *Ccl7*$^{-/-}$ B cells. Results are pooled from three independent experiments with 10–25 mice per group. (**b**,**c**) Representative photomicrographs (left) and quantitative analysis (right) of infarct size (**b**) and fibrosis and collagen content (**c**) in the indicated groups of mice. Results are pooled from three independent experiments with 10–25 mice per group. Mean values ± s.e.m. are shown. Scale bars: 1 mm in **b** and 100 µm in **c**. **P* < 0.05 and ****P* < 0.001 versus WT splenocytes; $^{\#}P$ < 0.05 and $^{\#\#\#}P$ < 0.001 versus anti-CD20 splenocytes; $^{\$}P$ < 0.05 and $^{\$\$\$}P$ < 0.001 versus anti-CD20 splenocytes with WT B cells. (**d**) Circulating Ccl7 protein concentrations at day 14 post-myocardial infarction in mice repopulated with a mixture of µMT and *Ccl7*$^{-/-}$ bone marrow compared to the control group receiving a mixture of µMT and *Ccl7*$^{+/+}$ bone marrow (*n* = 9–13 mice per group). ***P* < 0.01. (**e**) FS at day 14 after myocardial infarction in the indicated groups of mice (*n* = 9–13 mice per group). Mean values ± s.e.m. are shown. **P* < 0.05.

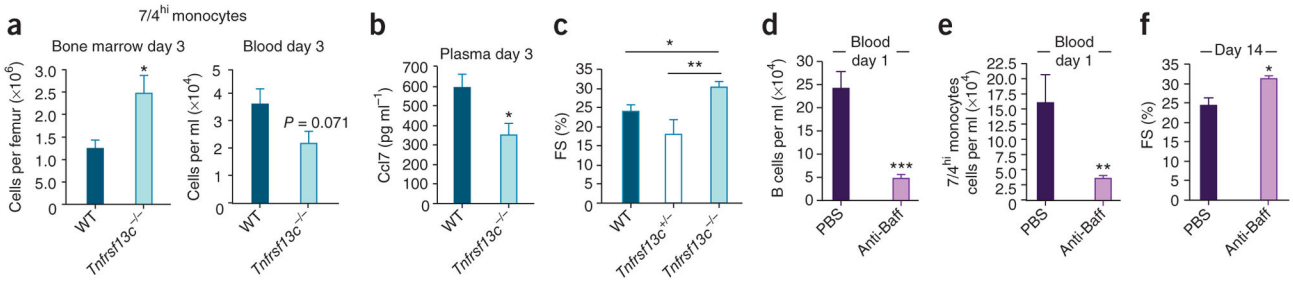

Figure 5.

Blockade of Baff signaling impairs monocyte mobilization and improves heart function after acute myocardial infarction. (**a**) Quantification of the number of 7/4^{hi} monocytes in the bone marrow (left) and in the blood (right) of Baff-r deficient (*Tnfrsf13c*$^{-/-}$) and WT control mice compared to controls on day 3 after myocardial infarction (*n* = 8–11 mice per group). (**b**) Ccl7 protein concentration in the plasma of *Tnfrsf13c*$^{-/-}$ mice compared to controls at day 3 after myocardial infarction (*n* = 8–11 mice per group). (**c**) FS of *Tnfrsf13c*$^{-/-}$ mice compared to *Tnfrsf13c*$^{+/+}$ and *Tnfrsf13c*$^{+/-}$ mice at day 14 after myocardial infarction. *n* = 8–11 mice per group. Mean values ± s.e.m. are shown. **P* < 0.05 and ***P* < 0.01. (**d**,**e**) Numbers of B220^{+}IgM^{+} B cells (**d**) and 7/4^{hi} monocytes (**e**) in blood of anti-Baff–treated mice compared to PBS-injected mice at day 1 after myocardial infarction (*n* = 8–11 mice per group). (**f**) FS of anti-Baff–treated mice compared to PBS-injected mice at day 14 after myocardial infarction (*n* = 12–15 mice per group). **P* < 0.05, ***P* < 0.01, ****P* < 0.001. Error bars indicate s.e.m.

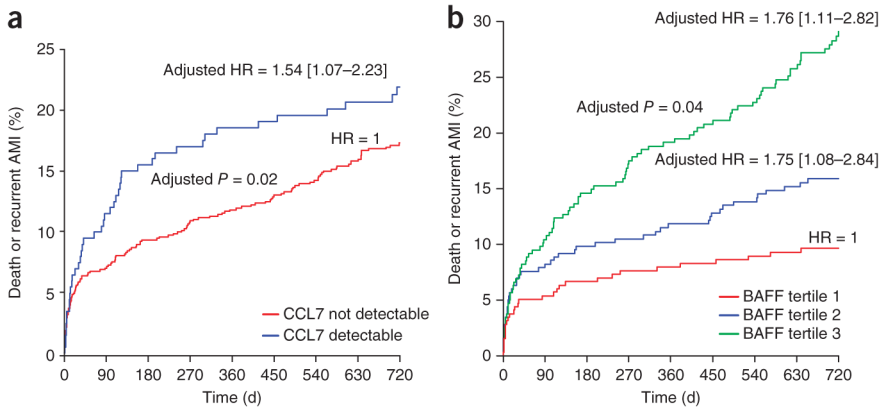

Figure 6.

Circulating levels of CCL7 and BAFF during the acute phase of myocardial infarction are associated with cardiovascular outcomes. (**a**,**b**) The probability of outcome events (death or recurrent myocardial infarction) as a function of baseline circulating CCL7 (**a**) or BAFF (**b**) levels in patients with acute myocardial infarction (AMI). HR, hazard ratio.